Published in final edited form as:
J Mol Cell Cardiol. 2009 December ; 47(6): 835–845. doi:10.1016/j.yjmcc.2009.08.017.

Beneficial Effects of Soluble Epoxide Hydrolase Inhibitors in Myocardial Infarction Model: Insight Gained Using Metabolomic Approaches

Ning Li[1], **Jun-Yan Liu**[3], **Valeriy Timofeyev**[1], **Hong Qiu**[1], **Sung Hee Hwang**[3], **Dipika Tuteja**[1], **Ling Lu**[1], **Jun Yang**[3], **Hideki Mochida**[1], **Reginald Low**[1], **Bruce D. Hammock**[3], and **Nipavan Chiamvimonvat**[1,2]

[1]Division of Cardiovascular Medicine University of California, Davis Davis, CA

[2]Department of Veterans Affairs, Northern California Health Care System Mather, CA

[3]Department of Entomology and UCD Cancer Research Center, University of California, Davis, CA

Abstract

Myocardial infarction (MI) leading to myocardial cell loss represents one of the common causes leading to cardiac failure. We have previously demonstrated the beneficial effects of several potent soluble epoxide hydrolase (sEH) inhibitors in cardiac hypertrophy. sEH catalizes the conversion of epoxyeicosatrienoic acids (EETs) to form the corresponding dihydroxyeicosatrienoic acids (DHETs). EETs are products of cytochrome P450 epoxygenases that have vasodilatory properties. Additionally, EETs inhibit the activation of nuclear factor (NF)-κB-mediated gene transcription. Motivated by the potential to uncover a new class of therapeutic agents for cardiovascular diseases which can be effectively used in clinical setting, we directly tested the biological effects of sEH inhibitors (sEHIs) on the progression of cardiac remodeling using a clinically relevant murine model of MI. We demonstrated that sEHIs were highly effective in the prevention of progressive cardiac remodeling post MI. Using metabolomic profiling of the inflammatory lipid mediators, we documented a significant decrease in EETs/DHETs ratio in MI model predicting a heightened inflammatory state. Treatment with sEHIs resulted in a change in the pattern of lipid mediators from one of inflammation towards resolution. Moreover, the oxylipin profiling showed a striking parallel to the changes in inflammatory cytokines in this model. Our study provides evidence for a possible new therapeutic strategy to improve cardiac function post MI.

INTRODUCTION

Cardiovascular disease is the leading cause of morbidity and mortality in the Western societies [1]. The incidence and prevalence of cardiac failure are increasing secondary to progressive aging of the population [2]. Once heart failure develops, the condition currently

Address for correspondence: Nipavan Chiamvimonvat Division of Cardiovascular Medicine, University of California, Davis One Shields Avenue, GBSF 6315 Davis, CA 95616 fax: (530) 752-3264 nchiamvimonvat@ucdavis.edu.

COMPETING INTERESTS STATEMENT NC and BDH have filed patents for the University of California for sEH and cardiac hypertrophy therapy. BDH founded Arete Therapeutics to move sEH inhibitors into clinical trials.

is irreversible and is associated with a very high mortality rate. Moreover, cardiac failure is associated with an increase in cardiac arrhythmias and sudden cardiac death.

We have previously documented beneficial effects of several potent soluble epoxide hydrolase (sEH) inhibitors (sEHIs) [3-5] in cardiac hypertrophy [6]. Indeed, sEH enzyme belongs to a relatively unexplored pathway of inflammatory lipid mediators which is mediated by cytochrome P450 enzymes, transforming arachidonic and linoleic acids to various biologically active compounds, including epoxyeicosatrienoic acids (EETs) or hydroxyeicosatrienoic acids (HETEs) and epoxyoctadecenoic acids (EpOMEs), respectively. EETs and EpOMEs are further metabolized by sEH to their corresponding diols, dihydroxyeicosatrienoic acids (DHETs) and dihydroxyoctadecenoic acids (DHOMEs), respectively [7, 8]. EETs have vasodilatory properties similar to that of endothelium-derived hyperpolarizing factor (EDHF) [9]. In addition, EETs produce an anti-inflammatory effect, at least in part, by inhibiting the activation of nuclear factor (NF)-κB-mediated gene transcription [10, 11].

Specifically, we have previously shown that administration of sEHIs results in the inhibition of cardiac hypertrophy [6]. We were able to demonstrate that these compounds block the activation of NF-κB in cardiac myocytes. Here, we tested the biological effects of sEHIs on the progression of cardiac remodeling using a clinically relevant murine model of myocardial infarction (MI). We demonstrate that the compounds are very effective in the prevention of progressive deterioration towards cardiac failure post MI. We further demonstrate that these compounds were highly effective in the prevention of cardiac arrhythmias which occur post MI.

Additionally, we further used metabolomic profiling to quantify lipid mediators in the model. Metabolomics represents the systematic study of the unique chemical fingerprints that result from cellular processes and metabolome embodies the collection of all metabolites in a biological organism, which are the end products of its gene expression. Hence, metabolic profiling can provide an instantaneous snapshot of the physiology of a particular cell. Indeed, using metabolomic profiling of the inflammatory lipid mediators, we documented a significant decrease in EETs/DHETs ratio in MI model predicting a heightened inflammatory state. Moreover, the oxylipin profiling showed a striking parallel to the changes in inflammatory cytokines. Finally, metabolomic profiling further provides important insights into the beneficial actions of sEHIs in this clinically relevant model.

METHODS

The investigation conforms with the Guide for the Care and Use of Laboratory Animals published by the US National Institutes of Health (NIH Publication No. 85-23, revised 1996) and were approved by the University of California, Davis Institutional Animal Care and Use Committee.

sEH inhibitors (sEHIs)

Two sEHIs, 1-adamantan-1-yl-3-{5-[2-(2-ethoxy-ethoxy)-ethoxy]-pentyl}-urea (AEPU)[5] and *trans*-4-[4-(3-adamantan-1-yl-ureido)-cyclohexyloxy]-benzoic acid (*t*-AUCB) were used in the study (see Fig. 1a for the structure of the compounds). The synthesis, physical properties, and spectral characteristics of AEPU and *t*-AUCB were synthesized in our laboratory as previously described [6, 12]. Measurement of water solubility and plasma concentration of the sEHIs is presented in the Online Data Supplement.

Myocardial infarction model in mice

A total of 76 male, wild type, 10~13 week-old C57Bl/6J mice were used. Eight mice died in the perioperative period. 7 mice were excluded from the study because of failure of the coronary occlusion, leaving a total of 61 mice in the study.

Myocardial infarction (MI) model in mice (ischemia/reperfusion) was created using procedure as described [13] using 45 minutes of ischemia and followed for a period of 3 weeks. Mice were randomized 3 days before surgery to receive two different sEHIs (Fig. 1**a**), AEPU in drinking water (100 mg/L) or *t*-AUCB (15 mg/L)[12] in the drinking water or water alone.

Morphometric and histological analyses

Cardiac sections were stained with Masson's trichrome. The % infarcted area represents the ratio of connective tissues to total LV area and was calculated by computerized planimetry (NIH Image J) [14] and described in details in Online Data Supplement. Measurements were performed by an observer blinded to the treatment groups. Additional histologic studies were performed using Sirius Red to assess for collagen content.

Whole-Cell Patch-Clamp Recordings

Cardiac myocytes were isolated from left ventricular free wall (LVFW) remote from the infarcted area using protocol previously described for MI model in rats [15]. APs were recorded at room temperature using the perforated-patch technique as previously described [16]. All other experiments were performed using the conventional whole-cell patch-clamp technique at room temperature [17]. Additional details are presented in the Online Data Supplement.

Analysis of cardiac function by echocardiography

Echocardiograms to assess systolic function were performed using M-mode and two-dimensional measurements as described in the Online Data Supplement. Fractional shortening (FS), a surrogate of systolic function, was calculated from left ventricle dimensions as follows: FS = ((EDD-ESD)/EDD) x100%, where EDD and ESD represent end-diastolic and end-systolic dimension, respectively.

In vivo electrophysiologic studies in mice

In-vivo electrophysiologic studies *were* performed as previously described [18, 19]. Additional details are presented in the Online Data Supplement.

Metabolomic Profiling of Oxylipins

Plasma samples stored at −80 °C were thawed at room temperature. Oxylipin profiling was performed using a modification of a previously published method [4] and described in details in Online Data Supplement.

Measurement of Plasma Cytokine Levels

Plasma samples were collected 3 weeks after sham or MI operation and stored at −70 °C until assayed. Plasma cytokine levels were analyzed using a Cytometric Bead Array kit (CBA mouse inflammation kit, BD Biosciences) to measure the concentrations of Interleukin-6 (IL-6), Interleukine-1β (IL-1β), Interleukin-10 (IL-10), Monocyte Chemoattractant Protein-1 (MCP-1), Tumor Necrosis Factor-α (TNF-α) and Interleukin-12p70 (IL-12 p70). Data were analyzed using BD Cytometric Bead Array Analysis software (BD Immunocytometry Systems).

Terminal Deoxynucleotidyl Transferase-Mediated dUTP Nick-End Labeling (TUNEL)

Hearts from sham and treated as well as untreated mice were fixed 24-48 hours in 4% neutral-buffered paraformaldehyde and later subjected to paraffin embedding and serial sectioning (5-μm). *In situ* Cell Death Detection Kit, TMR red (Roche Diagnostics), was used for the detection of apoptotic cells (please also refer to details in Online Data Supplement)

Western Blot Analysis

Immunoblots were performed as previously described [16]. The following primary antibodies were used: 1) Polyclonal anti-sEH antibody (1:200 dilution) against affinity-purified recombinant human sEH was raised from rabbits as previously described [20], 2) Polyclonal anti-brain natriuretic peptide (a kind gift from Dr. Seubert's laboratory) and 3) Anti-GAPDH antibody (Sigma) was used as an internal loading control.

Statistical analysis

Statistical comparisons were analyzed by one way ANOVA followed by Tukey or Games-Howell tests for post hoc comparison. Statistical significance was considered to be achieved when $P<0.05$.

RESULTS

Beneficial effects of sEHIs in a murine model with myocardial infarction (MI)

We created MI in 10-week-old male C57Bl/6J mice (Charles River, Wilmington, MA) using previously described techniques [13]. Three days before surgery, mice were randomized to receive either one of the two sEH inhibitors (sEHIs, Fig. 1**a**): AEPU (100 mg/L)[5] or *t*-AUCB (15 mg/L)[12] in drinking water or no treatment and this exposure was continued for three weeks after the surgery. Measurement of plasma drug levels is presented in the Online Data Supplement. Fig. 1**a** shows structures of the two sEHIs used in the study. Fig. 1**b** shows photomicrographs of examples of whole hearts from MI mice treated with AEPU or *t*-AUCB in the drinking water for three weeks compared to MI alone or sham-operated hearts after three weeks of follow up. All MI mice showed evidence of an increase in chamber dilatation associated with myocardial infarct at follow up. In contrast, treatment with sEHIs resulted in a decrease in the infarct size and prevented the development of cardiac dilatation post MI. Summary data are shown in Fig. 1**c** illustrating a significant increase in the ratio of heart weight/tibial length (HW/TL) in the MI group compared to sham-operated hearts. In contrast, there were no significant changes in the HW/TL ratio in the MI groups treated with AEPU or *t*-AUCB compared to sham-operated controls.

Non-invasive assessment of cardiac function by echocardiography

We assessed the chamber size and systolic function in sham-operated and MI mice compared to MI mice treated with sEHIs using echocardiography. As shown in Fig. 2**a** using two-dimensional and M-mode echocardiography, treatment with AEPU or *t*-AUCB resulted in a significant improvement in LV systolic function associated with an improvement in chamber size. Summary data for the fractional shortening are shown in Fig. 2**c** and Table 1 depicting a significant improvement in fractional shortening of the MI mice treated with *t*-AUCB at three weeks of follow up compared to MI alone. Similar beneficial effects were observed after three-week treatment with AEPU (Fig. S1 in Online Data Supplement).

Left ventricular (LV) remodeling after MI

To directly quantify the degree of LV remodeling after MI, histologic analyses were performed. Fig. 2**b** shows histologic sections using Masson's trichrome stain from a sham-operated heart compared to MI hearts with or without treatment with *t*-AUCB. All MI mice

showed evidence of an increase in chamber dilatation associated with myocardial scars as previously described for this model [13, 21]. Treatment with *t*-AUCB resulted in a significant decrease in infarct size as well as a marked beneficial effect on the cardiac chamber remodeling. Direct quantification of the extent of connective tissues is presented in Fig. 3**a**, **c** showing a significant decrease in the percentage of infarcted area/total LV area in the treated group compared to MI alone. To further assess the degree of cardiac remodeling, we isolated single LV cardiac myocytes from LV free wall remote from the infarcted area as described in the Online Method. Additional histologic sections using Sirius Red stain for collagen are shown in Fig. S2 in Online Data Supplement. Fig. 3**b** shows representative photomicrographs of bright-field images of single isolated cardiac myocytes showing a significant increase in cell size in MI mice compared to sham animals. Treatment with sEHI resulted in a significant decrease in cell size. Cell size was further quantified using cell capacitance measurement with whole-cell patch-clamp techniques and summary data are shown in Fig. 3**d** illustrating a significant decrease in cell size in the treated group compared to MI alone (**P*<0.05). Hypertrophic marker was directly assessed using Western blot analyses and a polyclonal antibody directed against brain natriuretic peptide (BNP) (Fig. S3) showing an increase in BNP level in MI mice compared to sham animals. Treatment with t-AUCB for 3 weeks resulted in a decrease in the BNP to the control level. Similarly, treatment with t-AUCB for 3 weeks significantly increased the capillary density in the border zone in MI mice compared to MI alone (Fig. S4 in Online Data Supplement).

Prevention of cardiac arrhythmias in MI mice

We next performed *in vivo* electrophysiologic studies (EPS) in treated and untreated MI mice at three weeks as previously described [19] to test whether sEHIs have salutary effects on cardiac arrhythmias in the setting of chronic MI. Shown in Fig. 4**a** are examples of surface electrocardiogram and simultaneous intracardiac electrograms from atria and ventricles from MI mice showing inducible atrial and ventricular arrhythmias using programmed electrical stimulation. The susceptibility to increased atrial and ventricular arrhythmias was significantly suppressed in MI mice which had been randomized to the treatment with sEHIs. Summary data are shown in Table 1 in the Online Data Supplement.

Reversal of electrical remodeling in MI mice treated with sEHIs

We further examined the cellular basis for the increase propensity to cardiac arrhythmias by performing patch-clamp analysis using isolated cardiac myocytes. Action potentials (APs) were recorded using perforated patch-clamp techniques. APs were markedly prolonged in myocytes isolated from MI mice compared to those of sham animals (Fig. 4**b**). Moreover, treatment with sEHIs resulted in a significant reversal of the electrical remodeling (Fig. 4**b**). Summary data shows significant prolongation of AP duration (APD) at 90% repolarization (APD_{90}) in MI animals (Fig. 4**c**). Treatment with *t*-AUCB resulted in a significant decrease in APD_{90} compared to MI alone. In order to further investigate the basis for the cardiac AP prolongation observed in the MI animals, we next examined whole-cell transient outward K^+ current (I_{to}) from single LVFW myocytes from the three groups of animals. Panel **d** shows representative current traces elicited using a series of voltage-clamp steps from a holding potential of −80 mV. The observed prolongation in APD_{90} in the MI model was associated with a striking decrease in I_{to} (Fig. 4**d**). Treatment with *t*-AUCB resulted in a significant reversal of I_{to} down-regulation observed in the MI model. Panel **e** shows summary data for the current density-voltage relations of the peak I_{to} from three groups of animals. There was a significant decrease in the peak I_{to} in the MI group compared to sham-operated animals (*p<0.05). The decrease in I_{to} was partially reversed in the MI group treated with *t*-AUCB (*p<0.05 comparing MI with or without treatment with *t*-AUCB).

Metabolomic Profiling of the Inflammatory Lipid mediators Using Liquid Chromatograph/ Tandem Mass Spectroscopy (LC/MS/MS)

Treatment with *t*-AUCB significantly increased the levels of EETs. Specifically, the plasma levels of 14(15)-, 11(12)-, and 8(9)-EET in MI mice were 0.34±0.09, 0.26±0.07, and 0.24±0.08 nM, respectively. Note that 5(6)-EET is not stable during the analytical procedure and no 5(6)-EET data are reported. After administration of *t*-AUCB, the plasma levels of 14(15)-, 11(12)-, and 8(9)-EET increased significantly to 1.07±0.19, 0.5±0.15, and 0.54±0.14 nM, respectively (*$p<0.05$). In addition, treatment with *t*-AUCB increased the level of EETs in a similar manner in sham animals (*See Table 3 in Online Data Supplement*). This finding can be depicted more clearly by comparing ratios of EETs to DHETs. EETs are metabolized to respective DHETs in the presence of sEH, therefore, we further analyzed the ratios of epoxides to the respective diols as an indicator of sEH action (Fig. 5**a**). Importantly, MI resulted in a significant decrease in the plasma ratio of total EETs/DHETs (Sum EET/Sum DHET) as well as 11(12)-EET/11(12)-DHET and 14(15)-EET/14(15)-DHET compared to sham animals (Fig. 5**a**. *$p<0.05$). Treatment with *t*-AUCB in the MI animals resulted in a significant increase in the plasma ratios of total EETs/DHETs as well as 8(9)-EET/8(9)-DHET, 11(12)-EET/11(12)-DHET and 14(15)-EET/14(15)-DHET compared to MI alone (Fig. 5**a**, *$p<0.05$). There was also a significant increase in the plasma ratios of total EETs/DHETs as well as 8(9)-EET/8(9)-DHET and 14(15)-EET/14(15)-DHET comparing *t*-AUCB treated MI animals and sham-operated animals (Fig. 5**a**, *$p<0.05$). Figure 5**b** shows similar findings in EpOME/DHOME ratios. Complete analyses of oxylipins are presented in Table 2 & 3 of the Online Data Supplement. Additional oxylipin analyses in MI mice treated with AEPU, the second sEHI used in the study are shown in Fig. S4 in Online Data Supplement. Similar to t-AUCB, treatment with AEPU resulted in changes from inflammatory profile towards one with resolution.

Measurement of plasma inflammatory cytokines

To further investigate the mechanisms underlying the observed beneficial effects of sEHIs, plasma cytokine levels were analyzed following a three-week of follow up period (Fig. 5**c**). There was a significant increase in the levels of IFN-γ, MCP-1, IL-10 and IL-6 in the MI mice compared to sham animals, moreover, treatment with sEHIs resulted in the normalization of these cytokines compared to the untreated groups (*$p<0.05$). There was a trend toward an increase in the level of IL-12p70 in the MI animals compared to sham-operated animals, however, the difference was not statistically significant.

Assessment of cardiac apoptosis

Previous studies have suggested that the progressive deterioration in cardiac function post MI is associated with cellular apoptosis. To determine whether treatment with sEHIs may result in a beneficial effect *via* a reduction in cellular apoptosis, TUNEL was performed using hearts from four different groups of animals including MI and sham-operated animals with and without treatment with *t*-AUCB at three week of follow up (Fig. 6**a**). More than 2,000 myocytes from LV free wall distant from the infarct zone were analyzed by a blinded observer for each group of animals (a total of 3 animals were used from each group). TUNEL was significantly increased in MI mice compared to sham animals or MI treated with *t*-AUCB at three weeks after surgery. Specifically, the ratio of apoptotic to non apoptotic cells in the MI group was 0.7±0.1% while the ratios in the treated or untreated sham or treated MI groups were <0.001±0.0008% ($p<0.05$). Fig. 6**b** shows an example of a TUNEL-positive myocyte. These results suggest that the beneficial effect of sEHIs results at least in part in the decrease in progressive cardiac myocyte cell loss following MI.

Expression of sEH in the MI model

sEH has been documented to be highly expressed in liver and kidney. Moreover, we have previously documented a high level of expression of sEH in mouse atrial and ventricular myocytes. To directly test whether MI may up-regulate the sEH expression level, we performed Western blot using LVFW from sham, MI and MI animals treated with *t*-AUCB at 3 weeks. There were no significant differences in the sEH protein expression in sham, MI or MI animals treated with *t*-AUCB (Fig. 6**b**). As shown in Fig. 6**b**, both mouse ventricular tissues expressed a readily detectable level of sEH (detected as a single major band at a molecular mass of 60 kDa). However, there were no significant differences in the expression level in the three groups of animals.

DISCUSSION

Our present study provides new evidence that treatment with sEHIs can reduce infarct size and chronic cardiac remodeling post MI. Moreover, the use of sEHIs results in the prevention of electrical remodeling post MI and in so doing, prevents the propensity for the development of cardiac arrhythmias as assessed by *in vivo* electrophysiologic studies. We provide evidence that treatment with sEHIs result in a significant decrease in several inflammatory cytokines which are significantly elevated at 3 weeks post MI. Furthermore, we demonstrate that MI results in a significant decrease in EET/DHET and EpOME/DHOME ratios. The reversal in the elevation of cytokines levels by sEHIs is associated with the normalization of the ratios of EET/DHET and EpOME/DHOME in the MI model compared to untreated MI animals.

Mechanistic Insights into the Observed Beneficial Effects of sEHI in the MI model

Oxygenated lipids are collectively known as oxylipins. One of the most biologically important groups of oxylipins is the eicosanoids. Eicosanoids are potent modulators of immune responses and are derived from the 20-carbon atom arachidonic acid or similar fatty acids. The bulk of research and pharmaceutical industries have focused on the cyclooxygenase (COX) and lipoxygenase (LOX) pathways of arachidonic acid metabolisms. Indeed, the less explored pathway of cytochrome P450 enzymes can also transform arachidonic and linoleic acids to various biologically active compounds, including EETs or HETEs and EpOMEs, respectively. EETs and EpOMEs are further metabolized by sEH to their corresponding diols, DHETs and DHOMEs, respectively [7, 8].

EETs, generated mainly by enzyme CYP2J2 in the heart, have been shown to be cardioprotective [22]. All EET regioisomers show distinct vasodilatory actions, and function as endogenous hypotensive agents [23, 24]. It has been demonstrated that EETs promote postischemic functional recovery in isolated mouse hearts overexpressing *CYP2J2* gene [22, 25]. Indeed, recent human epidemiological studies have identified associations between variations in EETs metabolic pathway genes and increased cardiovascular risk. A polymorphism of the *CYP2J2* gene is associated with an increased risk of coronary artery disease [26], and *EPHX2* (encoding for sEH) has also been identified as a potential cardiovascular disease-susceptibility gene [27]. These findings provide evidence supporting the notion that EETs play a significant cardioprotective role in the heart. The underlying mechanisms of EET-mediated cardioprotection have only begun to be addressed. In general, when EETs are metabolized to DHETs by sEH, their biological activities become less pronounced [11]. Thus, when the elimination of EETs is suppressed by sEHIs, the steady-state cellular level of EETs increases *in vivo*, leading to cardioprotective effects in the setting of cardiac ischemia/reperfusion.

Both AEPU and t-AUCB are potent inhibitors of the sEH with half-blocking concentration (IC_{50}) in the low nanomolar range. The fact that these two inhibitors of sEH with radically different physical properties both yield similar outcome suggests that the inhibition of sEH is involved in the observed beneficial effects in MI.

We have previously documented using both *in vivo* and *in vitro* models that sEHIs can prevent the development of cardiac hypertrophy and block NF-κB activation [6]. NF-κB is inactive when bound to IκB, an inhibitory protein that is degraded by proteosomes when phosphorylated by IκB kinase (IKK) [28-30]. It has been shown that EETs inhibit IKK, preventing degradation of IκB. This maintains NF-κB in the inactive state and inhibits NF-κB-mediated gene transcription [10, 11]. Our present study provides direct evidence for the anti-inflammatory action of sEHIs by restoring EETs level as well as EET/DHET and EpOME/DHOME ratios in post MI model. The increase in the EETs level would be expected to prevent the amplification of inflammation by inhibiting the transcription factor NF-κB resulting in a reduction in inflammatory cytokines.

Metabolomic Analyses of the Inflammatory Lipid Mediators and Cytokines

Metabolomics analysis using LC/MS allows the monitoring of multiple plasma oxylipins, many of which are highly potent chemical mediators. As shown in Fig. 4**a**, the absolute levels of plasma EETs as well as the ratios of plasma EETs to their corresponding diols or DHETs increase in response to treatment with *t*-AUCB. This clearly indicates that levels of the sEHI were sufficiently high to engage the sEH target. Moreover, there was a significant decrease in the 11(12), 14(15) and total EET/DHET ratios when comparing MI mice to the sham animals suggesting that these ratios may be used as biomarkers of MI. This effect was in each case reversed by treatment with *t*-AUCB. These data are particularly significant because of the cardioprotective and anti-hypertensive roles of EETs [9, 31]. Similar conclusions can be drawn from the analysis of the linoleate series or 18:2 series of oxylipins. Linoleate epoxides are known as leukotoxin and isoleukotoxins (9(10)-EpOME and 12(13)-EpOME) and their diols as the corresponding DHOMEs. The higher concentration makes these materials easier to monitor than the EET/DHET series. Their biological activities are quite distinct from those of the EET/DHET pairs with the DHOMEs being proinflammatory mediators which increase vascular permeability. The same trends in terms of absolute amounts of epoxides and ratios of epoxides to diols were observed in the 18:2 linoleate series as were seen with the 20:4 arachidonate series. These findings further support our notion that the P450 epoxygenase–sEH metabolic pathway is being activated during MI and the effects can be reversed by treatment with sEHIs.

In addition, data from oxylipin analyses provide a striking parallel to the inflammatory cytokines in this model with and without treatment. Specifically, there was a significant increase in the levels of several inflammatory cytokines including IFN-γ, MCP-1, IL-10 and IL-6 in the MI mice compared to sham animals. Moreover, treatment with sEHIs resulted in the normalization of these cytokines compared to untreated groups. IL-6 plays a significant role in the development of acute inflammatory responses while the chemokine MCP-1 is a potent monocyte chemoattractant. Importantly, our findings indicate that treatment with sEHI increases EETs, EETs/DHETs and decreases inflammatory cytokines production.

On the other hand, TNF-α was not significantly altered in mouse MI model at 3 weeks. TNF-α is initially produced by resident monocytes and macrophages, is considered an early innate inflammatory mediator. It is possible that the sampling time may influence the findings. Further studies to follow the time course of the inflammatory cytokines as well as oxylipins analyses will likely provide additional important insights into the roles of inflammation in post MI remodeling. Indeed, oxylipins analyses may represent a new

"omics" approach to potentially gain additional insights into the inflammatory processes in cardiovascular diseases.

Finally, even though we have documented a decrease in the ratios of EETs/DHETs as well as EpOME/DHOMEs in MI model, there was no documented increase in the expression of sEH enzyme at the protein level at 3 week of follow up. Future studies to follow the time course of the level of expression during MI may be warranted to further assess the role of the enzyme sEH in the inflammatory process post MI.

Reversal of electrical remodeling

We demonstrated that sEHIs can prevent cardiac remodeling post MI. Moreover, we were able to demonstrate that the use of sEHIs can prevent the development of electrical remodeling and ventricular arrhythmias which occur post MI. The cellular electrophysiology in cardiac hypertrophy and failure has been extensively studied in a variety of animal models. The single most consistent abnormality found in these studies is APD prolongation. The prolongation was due at least in part to the reduction in the 4-aminopyridine-sensitive Ca^{2+}-independent transient outward K^+ current (I_{to}) [32]. Specifically, treatment with sEHI prevented the down-regulation of I_{to} and APD prolongation which occurs post MI.

Previous studies on the cardioprotective effects of sEHIs

The cardioprotective effects of sEHIs have drawn much attention in recent years. Several studies have documented the cardioprotective roles of sEH inhibition in myocardial ischemia-reperfusion injury using sEH knockout mice [33, 34] as well as a dog MI model [35]. On the other hand, these previous studies have provided evidence for the cardioprotective effects of sEHIs mainly in acute MI while our study support the beneficial effects of two different compounds with inhibitory effects on sEH over a follow-up period of 3 weeks after MI. Apart from the documented biological effects, we utilized LC/MS/MS to analyze a group of oxylipins and provided evidence for a significant decrease in EET/DHET and EpOME/DHOME ratios in MI mice, thus, providing rationale for the use of sEHIs in MI. The decrease in EET/DHET and EpOME/DHOME ratios was found to be associated with a significant increase in several inflammatory cytokines at 3 weeks post MI. Treatment with sEHIs resulted in the normalization of the ratios of EET/DHET and EpOME/DHOME in the MI model compared to untreated MI animals. This was associated with the reversal in the elevation of cytokines levels by sEHIs at 3 weeks post MI. Finally, the use of sEHIs results in the prevention of electrical remodeling post MI and in so doing, prevents the propensity for the development of cardiac arrhythmias as assessed by in vivo electrophysiologic studies.

Limitations of the Study

Our study demonstrates that sEHIs result in a reduction in infarct size from MI as well as prevention of cardiac remodeling post MI at 3 weeks of follow up. Additional study will be necessary to examine the effects of sEHIs on the structural and electrical remodeling independent of its effects on the reduction in infarct size. Moreover, since sEHIs are vasodilatory, the observed beneficial effects may be due to a decrease in afterload on the heart. Nonetheless, our previous study have documented an antihypertrophic effect of sEHIs on cardiac myocytes likely from the inhibition of NF-κB [6].

In summary, we have demonstrated the efficacy of orally administered and structurally diverse sEHIs in two separate murine models of cardiac hypertrophy and failure. From a basic perspective, the results indicate a need for a greater understanding of epoxylipids in cardiac biology. From a clinical perspective, the results suggest that epoxide containing lipid mediators, their mimics, sEHIs or combinations of these agents may retard or even reverse

cardiac hypertrophy and failure. Our study provides results on a class of new compound which could be used effectively in the setting of MI. Moreover, additional data from our laboratory suggest that sEHIs further transcriptionally downregulates COX2 enzyme of the cyclooxygenase pathway [36]. Hence, sEHIs may be predicted to act synergistically with COX inhibitor (e.g., aspirin) which is already used routinely in acute MI setting. Our study has important clinical significance in providing evidence for a novel alternative strategy in the treatment of cardiac failure and the prevention of ventricular arrhythmias associated with cardiac failure.

Supplementary Material

Refer to Web version on PubMed Central for supplementary material.

Acknowledgments

The authors acknowledge the UC Davis Health System (UCDHS) Confocal Microscopy Facility. Supported by the Department of Veteran Affairs Merit Review Grant and the National Institutes of Health Grants (HL85844, HL85727) to N.C. Partial supports were provided by NIEHS Grant R37 ES02710, the NIEHS Superfund Basic Research Program (P42 ES04699), the NIEHS Center for Children's Environmental Health & Disease Prevention (P01 ES11269) and a Technology Translational Grant from UCDHS.

REFERENCES

[1]. Rosamond W, Flegal K, Friday G, Furie K, Go A, Greenlund K, et al. Heart disease and stroke statistics--2007 update: a report from the American Heart Association Statistics Committee and Stroke Statistics Subcommittee. Circulation. Feb 6; 2007 115(5):e69–171. [PubMed: 17194875]

[2]. Frey N, Olson EN. Cardiac hypertrophy: the good, the bad, and the ugly. Annu Rev Physiol. 2003; 65:45–79. [PubMed: 12524460]

[3]. Morisseau C, Goodrow MH, Dowdy D, Zheng J, Greene JF, Sanborn JR, et al. Potent urea and carbamate inhibitors of soluble epoxide hydrolases. Proc Natl Acad Sci U S A. Aug 3; 1999 96(16):8849–54. [PubMed: 10430859]

[4]. Morisseau C, Goodrow MH, Newman JW, Wheelock CE, Dowdy DL, Hammock BD. Structural refinement of inhibitors of urea-based soluble epoxide hydrolases. Biochem Pharmacol. May 1; 2002 63(9):1599–608. [PubMed: 12007563]

[5]. Morisseau C, Hammock BD. Epoxide hydrolases: mechanisms, inhibitor designs, and biological roles. Annu Rev Pharmacol Toxicol. 2005; 45:311–33. [PubMed: 15822179]

[6]. Xu D, Li N, He Y, Timofeyev V, Lu L, Tsai HJ, et al. Prevention and reversal of cardiac hypertrophy by soluble epoxide hydrolase inhibitors. Proc Natl Acad Sci U S A. Dec 5; 2006 103(49):18733–8. [PubMed: 17130447]

[7]. Yu Z, Xu F, Huse LM, Morisseau C, Draper AJ, Newman JW, et al. Soluble epoxide hydrolase regulates hydrolysis of vasoactive epoxyeicosatrienoic acids. Circ Res. Nov 24; 2000 87(11): 992–8. [PubMed: 11090543]

[8]. Zeldin DC, Moomaw CR, Jesse N, Tomer KB, Beetham J, Hammock BD, et al. Biochemical characterization of the human liver cytochrome P450 arachidonic acid epoxygenase pathway. Arch Biochem Biophys. Jun 1; 1996 330(1):87–96. [PubMed: 8651708]

[9]. Spector AA, Norris AW. Action of epoxyeicosatrienoic acids on cellular function. Am J Physiol Cell Physiol. Mar; 2007 292(3):C996–1012. [PubMed: 16987999]

[10]. Campbell WB. New role for epoxyeicosatrienoic acids as anti-inflammatory mediators. Trends Pharmacol Sci. Apr; 2000 21(4):125–7. [PubMed: 10740283]

[11]. Node K, Huo Y, Ruan X, Yang B, Spiecker M, Ley K, et al. Anti-inflammatory properties of cytochrome P450 epoxygenase-derived eicosanoids. Science. Aug 20; 1999 285(5431):1276–9. [PubMed: 10455056]

[12]. Hwang SH, Tsai HJ, Liu JY, Morisseau C, Hammock BD. Orally bioavailable potent soluble epoxide hydrolase inhibitors. J Med Chem. Aug 9; 2007 50(16):3825–40. [PubMed: 17616115]

[13]. Tarnavski O, McMullen JR, Schinke M, Nie Q, Kong S, Izumo S. Mouse cardiac surgery: comprehensive techniques for the generation of mouse models of human diseases and their application for genomic studies. Physiol Genomics. Feb 13; 2004 16(3):349–60. [PubMed: 14679301]

[14]. Dawn B, Guo Y, Rezazadeh A, Huang Y, Stein AB, Hunt G, et al. Postinfarct cytokine therapy regenerates cardiac tissue and improves left ventricular function. Circ Res. Apr 28; 2006 98(8): 1098–105. [PubMed: 16556872]

[15]. Huang B, El-Sherif T, Gidh-Jain M, Qin D, El-Sherif N. Alterations of sodium channel kinetics and gene expression in the postinfarction remodeled myocardium. J Cardiovasc Electrophysiol. Feb; 2001 12(2):218–25. [PubMed: 11232622]

[16]. Xu Y, Zhang Z, Timofeyev V, Sharma D, Xu D, Tuteja D, et al. The effects of intracellular Ca^{2+} on cardiac K^+ channel expression and activity: novel insights from genetically altered mice. J Physiol. Feb 1; 2005 562(Pt 3):745–58. [PubMed: 15564282]

[17]. Hamill OP, Marty A, Neher E, Sakmann B, Sigworth FJ. Improved patch-clamp techniques for high-resolution current recording from cells and cell-free membrane patches. Pflugers Arch. 1981; 391(2):85–100. [PubMed: 6270629]

[18]. Berul CI, Aronovitz MJ, Wang PJ, Mendelsohn ME. In vivo cardiac electrophysiology studies in the mouse. Circulation. Nov 15; 1996 94(10):2641–8. [PubMed: 8921812]

[19]. Zhang Z, He Y, Tuteja D, Xu D, Timofeyev V, Zhang Q, et al. Functional Roles of $Ca_V1.3$ (α_{1D}) Calcium Channels in Atria. Insights Gained From Gene-Targeted Null Mutant Mice. Circulation. Sep 19.2005

[20]. Wixtrom RN, Silva MH, Hammock BD. Cytosolic epoxide hydrolase in human placenta. Placenta. Sep-Oct; 1988 9(5):559–63. [PubMed: 3222228]

[21]. Takimoto E, Champion HC, Li M, Belardi D, Ren S, Rodriguez ER, et al. Chronic inhibition of cyclic GMP phosphodiesterase 5A prevents and reverses cardiac hypertrophy. Nat Med. Feb; 2005 11(2):214–22. [PubMed: 15665834]

[22]. Seubert J, Yang B, Bradbury JA, Graves J, Degraff LM, Gabel S, et al. Enhanced postischemic functional recovery in CYP2J2 transgenic hearts involves mitochondrial ATP-sensitive K^+ channels and p42/p44 MAPK pathway. Circ Res. Sep 3; 2004 95(5):506–14. [PubMed: 15256482]

[23]. Roman RJ, Maier KG, Sun CW, Harder DR, Alonso-Galicia M. Renal and cardiovascular actions of 20-hydroxyeicosatetraenoic acid and epoxyeicosatrienoic acids. Clin Exp Pharmacol Physiol. Nov; 2000 27(11):855–65. [PubMed: 11071299]

[24]. Imig JD, Navar LG, Roman RJ, Reddy KK, Falck JR. Actions of epoxygenase metabolites on the preglomerular vasculature. J Am Soc Nephrol. Nov; 1996 7(11):2364–70. [PubMed: 8959626]

[25]. Nithipatikom K, Moore JM, Isbell MA, Falck JR, Gross GJ. Epoxyeicosatrienoic acids in cardioprotection: ischemic versus reperfusion injury. Am J Physiol Heart Circ Physiol. Aug; 2006 291(2):H537–42. [PubMed: 16473964]

[26]. Spiecker M, Darius H, Hankeln T, Soufi M, Sattler AM, Schaefer JR, et al. Risk of coronary artery disease associated with polymorphism of the cytochrome P450 epoxygenase CYP2J2. Circulation. Oct 12; 2004 110(15):2132–6. [PubMed: 15466638]

[27]. Lee CR, North KE, Bray MS, Fornage M, Seubert JM, Newman JW, et al. Genetic variation in soluble epoxide hydrolase (EPHX2) and risk of coronary heart disease: The Atherosclerosis Risk in Communities (ARIC) study. Hum Mol Genet. May 15; 2006 15(10):1640–9. [PubMed: 16595607]

[28]. Karin M. The beginning of the end: IkappaB kinase (IKK) and NF-kappaB activation. J Biol Chem. Sep 24; 1999 274(39):27339–42. [PubMed: 10488062]

[29]. Karin M. How NF-kappaB is activated: the role of the IkappaB kinase (IKK) complex. Oncogene. Nov 22; 1999 18(49):6867–74. [PubMed: 10602462]

[30]. Rothwarf DM, Karin M. The NF-kappa B activation pathway: a paradigm in information transfer from membrane to nucleus. Sci STKE. Oct 26.1999 1999(5):RE1. [PubMed: 11865184]

[31]. Spector AA, Fang X, Snyder GD, Weintraub NL. Epoxyeicosatrienoic acids (EETs): metabolism and biochemical function. Prog Lipid Res. Jan; 2004 43(1):55–90. [PubMed: 14636671]

[32]. Nabauer M, Kaab S. Potassium channel down-regulation in heart failure. Cardiovasc Res. Feb; 1998 37(2):324–34. [PubMed: 9614489]

[33]. Seubert JM, Sinal CJ, Graves J, DeGraff LM, Bradbury JA, Lee CR, et al. Role of soluble epoxide hydrolase in postischemic recovery of heart contractile function. Circ Res. Aug 18; 2006 99(4):442–50. [PubMed: 16857962]

[34]. Motoki A, Merkel MJ, Packwood WH, Cao Z, Liu L, Iliff J, et al. Soluble epoxide hydrolase inhibition and gene deletion are protective against myocardial ischemia-reperfusion injury in vivo. Am J Physiol Heart Circ Physiol. Nov; 2008 295(5):H2128–34. [PubMed: 18835921]

[35]. Gross GJ, Gauthier KM, Moore J, Falck JR, Hammock BD, Campbell WB, et al. Effects of the selective EET antagonist, 14,15-EEZE, on cardioprotection produced by exogenous or endogenous EETs in the canine heart. Am J Physiol Heart Circ Physiol. Jun; 2008 294(6):H2838–44. [PubMed: 18441205]

[36]. Schmelzer KR, Kubala L, Newman JW, Kim IH, Eiserich JP, Hammock BD. Soluble epoxide hydrolase is a therapeutic target for acute inflammation. Proc Natl Acad Sci U S A. Jul 12; 2005 102(28):9772–7. [PubMed: 15994227]

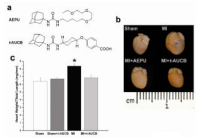

Fig. 1.

Beneficial effects of sEHIs (AEPU and *t*-AUCB) in a mouse MI model. **a**, Structure of the two sEHIs used in our studies: 1-adamantan-1-yl-3-{5-[2-(2-ethoxy-ethoxy)-ethoxy]-pentyl}-urea (AEPU, 100 mg/L)[5] and *trans*-4-[4-(3-adamantan-1-yl-ureido)-cyclohexyloxy]-benzoic acid (*t*-AUCB). **b,** Examples of whole hearts from MI mice treated with AEPU or *t*-AUCB compared to MI alone or sham-operated hearts. The mice were sacrificed after three weeks of follow up. Scale, 1 cm. **c**, Summary data for heart/tibial length ratios (mg/mm) from MI mice compared to untreated MI mice. Error bars are ± s.e.m. (n = 12). *$p<0.05$. Similar results were obtained with AEPU.

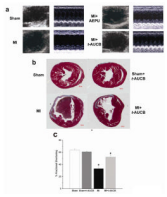

Fig. 2.

a, Examples of two-dimensional and M-mode echocardiography in mouse models with sham operation, MI and MI treated with AEPU or *t*-AUCB after three weeks of treatment showing evidence of cardiac failure with chamber dilatation in MI mice. AEPU and *t*-AUCB prevented the development of chamber dilatation in MI mice. **b**, Histologic sections (Masson's trichrome stain) of sham-operated and MI mouse hearts, showing infarct area with scarring and gross cardiac dilatation at 3 weeks in the MI mouse. Treatment of MI mice with *t*-AUCB in drinking water prevented the development of cardiac remodeling. All histologic cross sections are presented with right ventricles to the right. Scale bar, 100 μm. **c**, Summary data for % fractional shortening (FS). Data shown are mean ± s.e.m., n = 12 for each group, $^{*}p<0.05$ comparing MI and sham animals, $^{\#}p<0.05$ comparing treated *vs.* untreated MI animals.

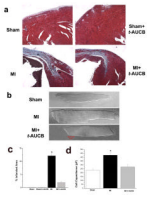

Fig. 3. Quantification of LV remodeling after MI using histologic analysis and whole-cell capacitance

a, Histologic sections (Masson's trichrome stain) of LV anterior wall of sham-operated and MI mouse hearts, showing connective tissues in blue. **b**, Representative photomicrographs of bright-field images of single isolated LV cardiomyocyte remote from infracted area. **c**, **d**, Summary data for % infracted area and cell capacitance, respectively. Data shown are mean ± s.e.m., n = 12 mice for each group, $^{*}p<0.05$. Similar data were obtained with AEPU.

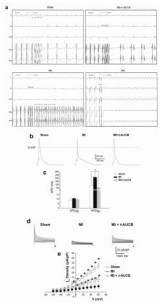

Fig. 4. Prevention of cardiac arrhythmia inducibility and electrical remodeling in MI mice by sEH inhibitors

a, *In-vivo* EPS in sham and treated compared to untreated MI animals. Sham and treated MI animals are shown in the upper panels. Lower panels are from untreated MI animals showing evidence of inducible atrial fibrillation (lower left panel) and ventricular tachycardia (lower right panel). Upper four tracing are surface ECG (Lead I, II and aVF). Lower two tracings are intracardiac electrogram showing atrial, and ventricular electrograms. Summary data are presented in *Supplemental Table 1*. **b,** Examples of AP recordings from LV free wall myocytes isolated from sham animals compared to treated and untreated MI animals at three weeks of follow up. APs recorded from MI mice were significantly prolonged compared to sham animals. Treatment with *t*-AUCB resulted in the normalization of the AP prolongation. Summary data for APD at 50 and 90% repolarization (APD_{50} and APD_{90} in ms) are shown in Panel **c**. (*$p<0.05$ comparing sham and treated MI animals to MI alone, n=12-15 cells for each group). **d,** Examples of Ca^{2+}-independent outward K^+ current traces elicited from a holding potential of −80 mV using test potentials of 2.5 seconds in duration from −60 to +60 mV in 10-mV increments. **e,** Summary data for the density of the peak outward components (*$p<0.05$ comparing sham and treated MI animals to MI alone). n=11-13 cells for each group.

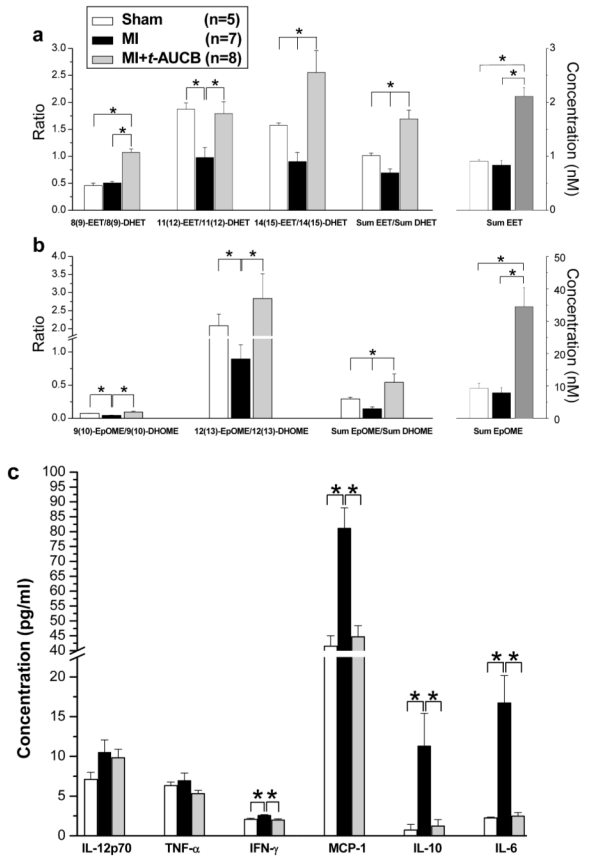

Fig. 5. Plasma Levels of Selected Oxylipin and Cytokines

a, b, Oxylipin profiling from sham, MI and MI treated with *t*-AUCB at 3 weeks of follow up (*p<0.05 comparing sham or treated MI groups to MI alone). **c,** Serum concentrations (in pg/ml) of IL-12p70, TNF-α, IFN-γ, MCP-1, IL-10 and IL-6 from sham, MI and MI treated with *t*-AUCB at 3 weeks of follow up (*p<0.05 comparing sham or treated MI groups to MI alone). See supplementary materials for full oxylipin profile.

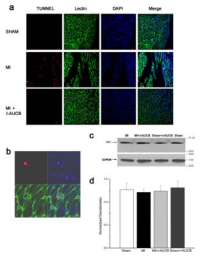

Fig. 6. Terminal Deoxynucleotidyl Transferase-Mediated dUTP Nick-End Labeling (TUNEL) and Western blot analysis

a, *In situ* cell death detection kit was used for the detection of apoptotic cells. Three independent experiments were performed. TUNEL-positive cells were visualized using a confocal microscope. **b,** An example of a TUNEL-positive myocyte (red) was shown with cardiac myocyte membranes (green) and nuclei (blue). The fraction of apoptotic cells was determined by dividing the number of TUNEL-positive cells (red) by the total number of DAPI-positive cardiac myocyte nuclei (blue). **c,** Immunoblots showing sEH protein from LV free wall in four different groups of animals; treated and untreated sham and MI. GAPDH protein was used as an internal loading control. **d,** Summary data showing the densitometry of sEH protein level normalized to GAPDH level in the four groups of animals.

Table 1

Summary of Echocardiographic Data

Treatment	N	EDD (cm)	ESD (cm)	LVPW (D) (cm)	LVPW (S) (cm)	FS (%)
Sham	6	0.31±0.02	0.13±0.01	0.09±0.01	0.16±0.01	64.2±2
Sham + *t*-AUCB	6	0.30±0.02	0.14±0.01	0.09±0.01	0.15±0.01	61.1±1
MI alone	11	0.36±0.02	0.25±0.02*	0.12±0.01	0.16±0.01	33.3±3*
MI + *t*-AUCB	11	0.34±0.02	0.16±0.02†	0.10±0.01	0.15±0.01	52.3±3†

EDD, end diastolic dimension; ESD, end systolic dimension; LVPW (D), left ventricular posterior wall thickness in diastole; LVPW (S), left ventricular posterior wall thickness in systole. Data are mean ±s.e.m. (one-way ANOVA Games-Howell test,

*p<0.05 comparing MI alone with sham,

†p<0.05 comparing treated vs. untreated MI animals).

J Mol Cell Cardiol. Author manuscript; available in PMC 2012 February 29.